

Improved Troposphere Blind Models Based on Numerical Weather Data

GREGOR MÖLLER, ROBERT WEBER, and JOHANNES BÖHM

Vienna University of Technology, Department of Geodesy and Geoinformation, Vienna, Austria

Received November 2013; Revised May 2014

ABSTRACT: *The troposphere blind model RTCA MOPS is the minimum operational performance standard for global positioning systems. With a standard deviation of 2.3% of the ZTD, it enables us to mitigate the main part of the tropospheric effect on GNSS signals. Nevertheless, the comparison of RTCA MOPS with modern troposphere models like the ESA model or GPT2 shows the limitation of RTCA MOPS and points out the potential of modern troposphere blind models based on climatological series derived from numerical weather data. The ESA model profits from a more advanced wet delay model and a higher spatial resolution. GPT2 shows the smallest mean bias on surface level in comparison to ray-tracing and IGS data and profits from additional mapping function coefficients – especially if the user is interested in tropospheric delay at low elevation angles. A revision of GPT2 - called GPT2w - combines the benefits of both aforementioned models. Copyright © 2014 Institute of Navigation.*

TROPOSPHERE CORRECTION MODELS

When passing the neutral atmosphere (in particular the troposphere, the lowest layer of the atmosphere) GNSS signals experience a path delay dependent on the variation of the refractive index due to temperature, pressure, and water vapor content. The tropospheric delay can reach up to a few tens of meters for very low elevation angles. Hence, it is a limiting factor for most space geodetic applications.

Several troposphere correction models have been developed to mitigate the tropospheric effect on GNSS signals. The troposphere blind model RTCA MOPS developed by Collins in 1999 [1] is the recommended troposphere model for Satellite-based Augmentation Systems (SBAS). RTCA MOPS [2] is based on a set of tabulated climatological data (pressure of air p , temperature T , water vapor pressure e , temperature lapse rate α , and vapor pressure decrease factor λ) and therewith is easy to implement and operable without any further information about the actual state of the atmosphere. The meteorological parameters are derived as mean values and annual amplitude from the U.S. Standard Atmosphere Supplements (1966). Its values are given in tabular form for five latitude belts (15°, 30°, 45°, 60°, and 75°). Variations of p , T , e , α ,

and λ are modeled as annual signals. The zenith hydrostatic delay at mean sea level (ZHD_0) is calculated by the formula of Saastamoinen [3].

$$ZHD_0[m] = 10^{-6} \cdot k_1 \cdot \frac{R_d \cdot p}{g_m} \quad (1)$$

where k_1 is the refraction coefficient for dry air (77.604 KhPa⁻¹), R_d is the constant of dry air (287.054 Jkg⁻¹K⁻¹), g_m is the mean gravity (9.784 ms⁻²) and p is the pressure of air at mean sea level in hPa.

The zenith wet delay (ZWD_0) at mean sea level can be obtained by the modified approach of [4].

$$ZWD_0[m] = \frac{10^{-6} \cdot k_3 \cdot R_d}{g_m \cdot (\lambda + 1) - \alpha \cdot R_d} \cdot \frac{e}{T} \quad (2)$$

where k_3 is a refraction coefficient for wet air (382000 K²hPa⁻¹), e is the water vapor pressure at mean sea level (hPa), λ is the vapor pressure decrease factor (dimensionless), α is the temperature lapse rate (Km⁻¹), and T is the temperature at mean sea level (K), see [4]. For reduction to the receiver height H (above mean sea level) the following formulas are applied:

$$ZHD[m] = \left(1 - \frac{\alpha \cdot H}{T}\right)^{\frac{g}{R_d \cdot \alpha}} \cdot ZHD_0 \quad (3)$$

$$ZWD[m] = \left(1 - \frac{\alpha \cdot H}{T}\right)^{\frac{(\lambda+1)g}{R_d \cdot \alpha} - 1} \cdot ZWD_0 \quad (4)$$

where g is the acceleration of the gravity (9.80665 ms⁻²).

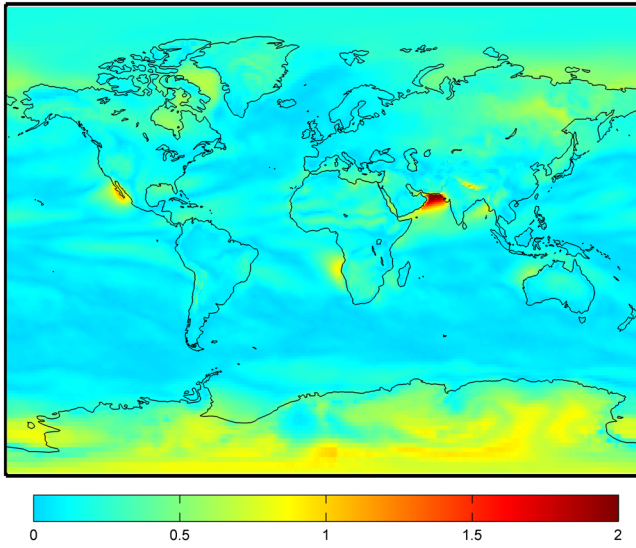


Fig. 1–Semi-annual amplitude of the water vapor decrease factor. The regions in red and yellow benefit from the additional semi-annual harmonics of GPT2 and GPT2w

To obtain the slant tropospheric delay (*STD*) the zenith hydrostatic and wet delays are mapped down to any elevation angle E_i by the rather simple mapping function $mf(E_i)$ developed by Black and Eisner [5].

$$STD(E_i) = (ZHD + ZWD) \cdot mf(E_i) \quad (5)$$

$$mf(E_i) = \frac{1.001}{\sqrt{0.002001 + \sin(E_i)^2}} \quad (6)$$

A more advanced troposphere model is the ESA blind model; see [6]. It is based on the same models for ZHD and ZWD as RTCA MOPS but profits from an improved climatological dataset and a more precise mapping function. The five model input parameters (pressure p , mean temperature T_m , mean temperature lapse rate α_m , water vapor pressure e , and water vapor pressure decrease factor λ) are derived by ERA-15 [7] statistical analysis and stored on a global grid with a spatial resolution of $1.5^\circ \times 1.5^\circ$. In contrast to RTCA MOPS, the refractivity coefficient k_3 is redefined, the temperature lapse rate α is replaced by T_m and the gravity acceleration g_m is not a constant anymore but rather a function of latitude and height of the receiver above mean sea level. In total 21 maps are used to build the climatological dataset. This includes the average value, annual fluctuation, and day of the minimum value for all five input parameters. For T_m , λ , and e in addition daily fluctuation and the hour of the day at which the minimum value occurs are stored.

The vertical extrapolation in the ESA model is realized on parameter-level, i.e., T_m , p , and e are extrapolated to receiver height, where the required additional parameters T_s (air temperature at surface) and α are derived from the given input parameters T_m , λ , and α_m . The horizontal interpolation of the tropospheric delay is done by bilinear interpolation between the neighboring four grid points. To obtain the tropospheric delay for any elevation angle the Niell mapping function [8]

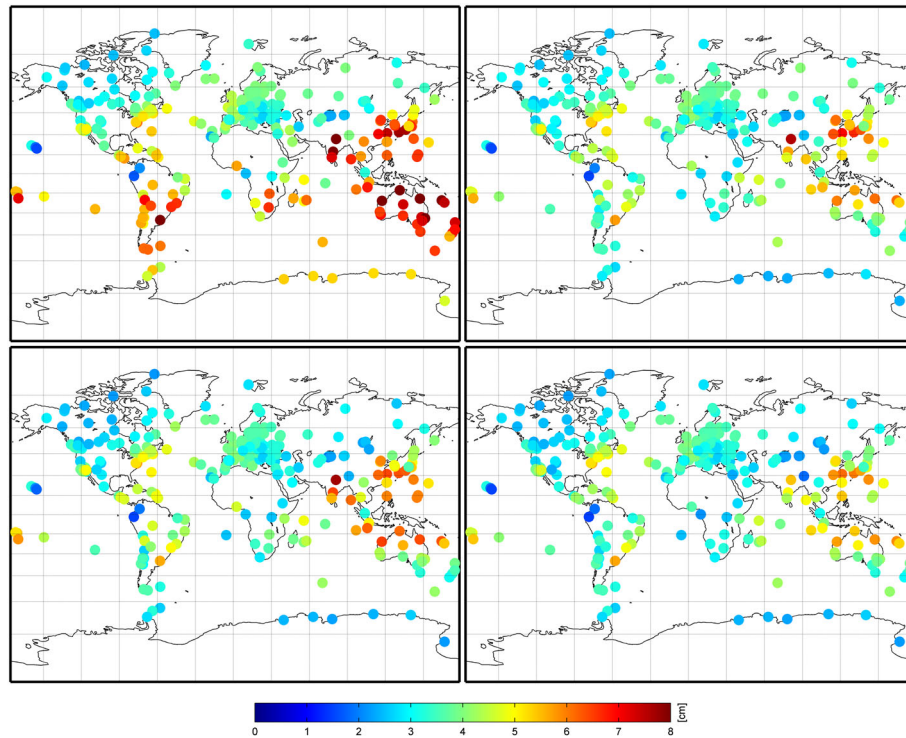


Fig. 2–Standard deviation of the differences between IGS ZTDs and model ZTDs [cm] derived from IGS minus RTCA MOPS (top left), ESA model (top right), GPT2 (bottom left) and GPT2w (bottom right) – calculated for ~320 IGS sites over the period 2012

Table 1—Overview of troposphere blind models

Blind model	temporal resolution	spatial resolution	parameter	hydrostatic delay model	wet delay model	mapping function
RTCA MOPS	annual	15°	p, T, e, α, λ	Saastamoinen [3]	Askne & Nordius [4]	Black & Eisner [5]
ESA model	daily + annual	1.5°	$p, T_m, \alpha_m, e, \lambda$	Saastamoinen [3]	Askne & Nordius [4]	Niell [8]
GPT2	annual + semi-annual	5°	p, T, Q, dT, a_h, a_w	Saastamoinen [3]	Saastamoinen [3]	GPT2 [9]
GPT2w	annual + semi-annual	1°	$p, T, T_m, dT, Q, \lambda, a_h, a_w$	Saastamoinen [3]	Askne & Nordius [4]	GPT2 [9]

Table 2—Bias and standard deviation of the differences between ZTDs delivered by CDDIS (<ftp://cddis.nasa.gov/gps/products/troposphere/zpd>) and blind models – for the period 2012

	RTCA MOPS	ESA model	GPT2	GPT2w
bias	-2.6 cm	0.8 cm	-0.4 cm	0.0 cm
min	-28.5 cm	-35.5 cm	-29.2 cm	-26.7 cm
max	19.8 cm	26.2 cm	28.0 cm	27.0 cm
σ	5.8 cm	4.1 cm	5.0 cm	4.1 cm

is applied - separately for the hydrostatic and wet part of the tropospheric delay.

The tropospheric model GPT2 [9] is an enhancement of the Global Pressure and Temperature model [10, 11] and the Global Mapping Function [12, 13]. The development and validation of GPT2 as well as the comparison with GPT/GMF have been described in detail by Lagler in [9]. In its current version, ZHD and ZWD are a function of air pressure, temperature, water vapor pressure, latitude, and ellipsoidal height. The internally derived parameters (p, T, Q, dT, a_h , and a_w) are obtained from the statistical analysis of monthly mean ERA-Interim profiles over the time period 2001 to 2010. They are stored as average value as well as amplitude of annual and semi-annual variations on a global grid with a resolution of $5^\circ \times 5^\circ$.

In contrast to the ESA model, the wet delay in GPT2 is only a function of e and T . The water vapor

pressure e is calculated from pressure p and the specific humidity Q . Internally stored dry and wet mapping function coefficients a_h and a_w help to reduce the mapping function error - especially for low elevations.

The GPT2 height scaling of the surface values T, p , and e is realized by means of the temperature lapse rate dT , mean gravity g_m (9.80665 ms^{-2}) and virtual temperature T_v , - derived from the given input parameters T and Q . The horizontal interpolation is done in a bilinear scheme on the parameter-level, i. e., GPT2 delivers meteorological parameters for any receiver location.

An enhancement of GPT2 - called GPT2w - is currently under development. The extension 'w' is related to the new wet delay model and the additional parameters λ and T_m which are provided as average value as well as amplitude of annual and semi-annual variations on a global one degree grid. The semi-annual harmonics allow us to take the characteristic of the tropical and subtropical climates into account, which are dominated by semi-annual rain periods; see Figure 1. The retrieval of λ from numerical weather models or radiosonde data is tricky, because the distribution of water vapor with height is rather irregular, yielding to unrealistic - or at least not practical - values. For GPT2w we have used global grids of ZWDs (determined by ray-tracing), with T_m and e as determined from ERA-Interim data. Then we

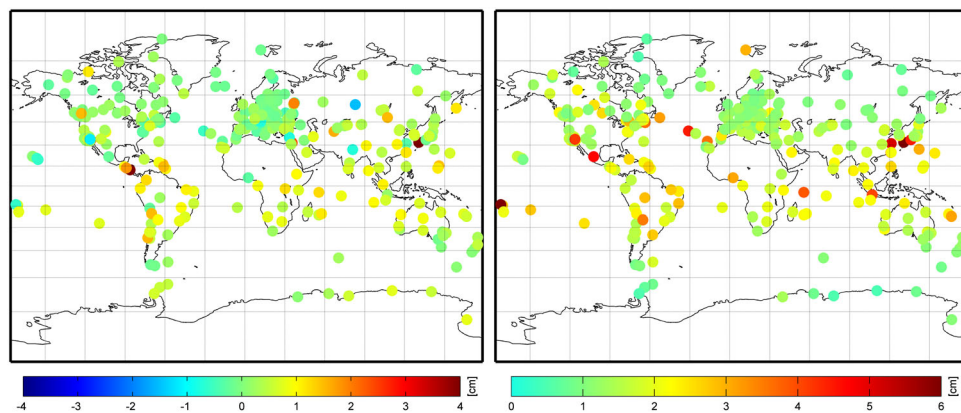


Fig. 3—Bias (left) and standard deviation (right) of the differences between IGS ZTDs and ray-tracing ZTDs [cm] - calculated for ~320 IGS sites over the period January 2013

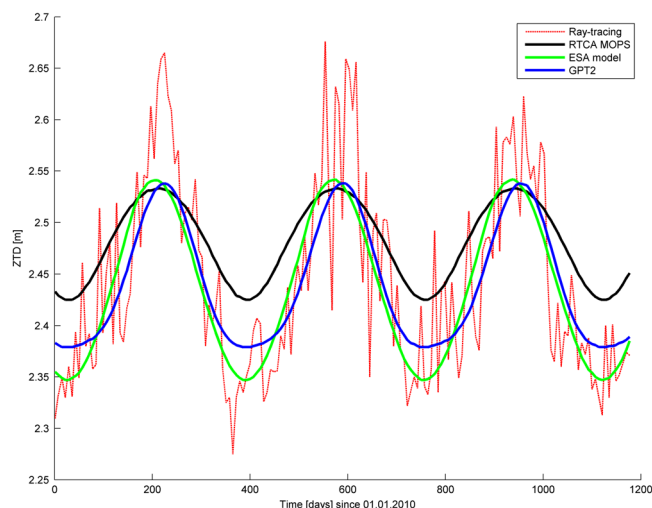


Fig. 4-ZTD [m] at station Tsukuba (Japan) derived from ray-tracing (red), RTCA MOPS (black), ESA model (green) and GPT2 (blue)

inverted the equation provided by [4] to derived global grids of λ . These values of λ are fully consistent with the zenith delays and thus do not result in unrealistic values. Consequently, those parameters are the best estimates for λ in terms of zenith wet delays. Therewith it will be possible to calculate the ZWD more reliably.

The main characteristics of the described tropospheric correction models are summarized in Table 1. In order to compare GPT2w with the others and to validate its performance, time series of ZWD, ZHD, and mapping parameters have been derived on a global grid as well as for a selection of about 320 GNSS sites. The validation is carried out with data delivered by the International GNSS Service (IGS) as well as operational model data from ECMWF.

VALIDATION BY IGS DATA

Since 2011 the United States Naval Observatory (USNO) has provided the final troposphere estimates for the IGS from observation data of more than 350 globally distributed GNSS sites [14]. The estimates are stored station-wise in daily files. Each file contains the zenith tropospheric delays (ZTD), the gradients in the north and east directions, and the corresponding formal error with a temporal resolution of 5 min. For further information about the processing strategy we refer the reader to [15].

For our validation campaign the ZTDs are extracted for the period 2012 and compared with the ZTDs derived from each troposphere correction model. IGS tropospheric delays with a formal error larger than 18 mm are excluded from the comparison. Figure 2 shows the standard deviation of the differences between IGS ZTDs and the ZTDs derived from the troposphere correction models RTCA MOPS, ESA model, GPT2, and GPT2w.

RTCA MOPS shows good agreement over Europe, North America, and parts of Asia but shows high

variations in almost every other region of the world. The bias of the differences - calculated for the period 2012 - varies between -29 cm and 20 cm (see Table 2), with the largest values over South America and Australia. The global bias is -2.6 cm, i.e., RTCA MOPS overestimates the ZTD significantly.

The residuals of the ESA model are in most cases smaller than the residuals of RTCA MOPS - especially in the eastern part of Asia and over the southern hemisphere. This leads to a reduced total standard deviation of 4.1 cm. Nevertheless, the differences vary between 26 cm and -36 cm with a maximum in the region of Indonesia and East China. The global bias is 8 mm, i.e., the ESA model underestimates the ZTD slightly.

The ZTD derived from GPT2 is in good agreement with the ZTD derived from IGS in higher latitudes. Its weakness is visible in the Asian Pacific region as well as in higher altitudes. This is rooted in the current ZWD model implemented in GPT2 which does not take the vertical distribution of the water vapor into account but assumes constant specific humidity with height. In consequence the standard deviation is with 5 cm (over all sites) about 9 mm larger than for the ESA model. Nevertheless, GPT2 shows almost no bias in comparison with IGS ZTDs.

The improvements of GPT2w (with respect to GPT2) are clearly visible. GPT2w profits from the higher spatial resolution of $1^\circ \times 1^\circ$, the improved wet delay model by Askne and Nordius [4], the new parameter T_m and λ as well as the improved method to calculate the water vapor partial pressure (e) from air pressure and water vapor decrease factor. With a standard deviation of 4.1 cm GPT2w performs on the same level as the ESA model - with small improvements visible in the Asian Pacific Region. In contrast to all other models, GPT2w shows no bias at all with respect to IGS ZTDs.

VALIDATION BY RAY-TRACING

The ECMWF provides a broad range of model products for various lead times (short range to seasonal scale) with different horizontal resolutions. In order to validate the troposphere correction models on a global grid, products from the operational model data sets from ECMWF are used to obtain reference delays with a temporal resolution of 6 hours on a global grid of $2.0^\circ \times 2.5^\circ$. Therefore the Vienna ray-tracer was applied through the pressure level data to obtain tropospheric delays for different elevation angles. A more detailed description of the Vienna ray-tracer can be found in [16].

The tropospheric delays derived by ray-tracing through ECMWF data and the estimated ZTD

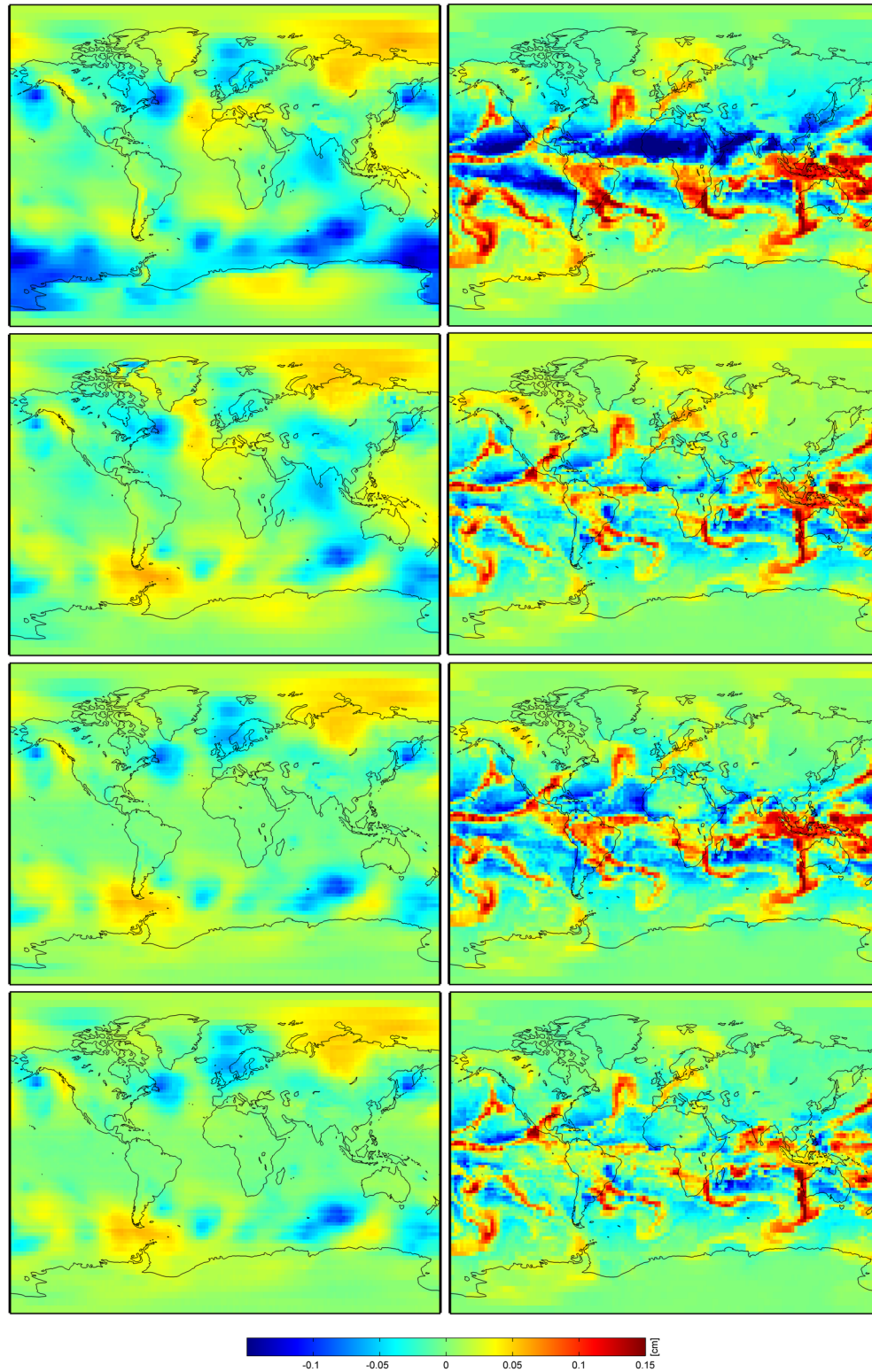


Fig. 5–Differences in ZHD (left column) and ZWD (right column) for January 1st, 2013, 0:00 UT [m]. Ray-tracing minus RTCA MOPS (top row), ESA model (2nd row), GPT2 (3rd row) and GPT2w (bottom row)

from IGS are sensitive to weather phenomena. Hence the residuals between both datasets are rather small (see Figure 3). The total bias (over all 320 sites) is 3 mm with an expected standard deviation of 1.6 cm. Thus, the quality of the ray-

tracing ZTDs is assumed to be comparable to that of the IGS ZTDs - especially over Europe, North America, and in higher latitudes.

Figure 4 shows the ZTD for the IGS site Tsukuba (Japan) derived by ray-tracing through

Table 3—Bias and Standard deviation between ray-tracing through 6 hourly operational pressure level data of ECMWF and the tropospheric delays derived by blind models – for the period January 2013

Blind model	ZHD		ZWD		ZTD	
	bias	σ	bias	σ	bias	σ
RTCA MOPS	-0.6 cm	3.0 cm	-0.5 cm	5.5 cm	-1.2 cm	5.5 cm
ESA model	0.3 cm	2.0 cm	0.5 cm	3.9 cm	0.8 cm	4.2 cm
GPT2	0.2 cm	1.9 cm	0.0 cm	4.3 cm	0.2 cm	4.5 cm
GPT2w	0.2 cm	1.9 cm	0.0 cm	3.6 cm	0.2 cm	3.9 cm

ERA Interim data, RTCA MOPS, the ESA model, and GPT2 over a period of three years. It can be seen that tropospheric blind models cannot describe real weather phenomena, but they can model regular variations like annual or semi-annual variations. The meteorological parameter of GPT2 and the ESA model are derived from numerical weather data, hence they fit the ray-tracing better than RTCA MOPS.

Ray-tracing allows us to separate the wet delay from the hydrostatic delay. Thus it is possible to validate ZHDs and ZWDs – derived from each tropospheric model – independently. Figure 5 shows the differences in ZHD and ZWD for January 1, 2013, 0:00 UT on a global grid. RTCA MOPS does not allow for taking longitude-dependent effects into account. Furthermore, it does not distinguish between northern and southern hemisphere and assumes a fixed day of maximum winter which leads to a higher bias and standard deviation (see Table 3). The main differences in ZHD are visible in higher latitudes (with the largest biases over the Southern Ocean and Northeast Russia). The largest wet bias of RTCA MOPS appears in the tropic and subtropic region like over Africa, the Arabian Sea, South America and parts of the Asian pacific region. This widely confirms the results presented in [17], especially the aridness not reflected over North Africa which was also found in the previous analysis.

The ESA model and GPT2 show similar characteristics to RTCA MOPS over northern latitudes but with significantly smaller bias and smaller standard deviation. Over the southern latitudes and North Africa both models benefit from the more advanced meteorological parameter set – derived from numerical weather data. If only the ZHD is of interest for the user, GPT2 performs slightly better than the ESA model. On the other hand, if in addition the ZWD or the ZTD is needed, GPT2 suffers from the simplified wet delay model and the lower spatial resolution. Especially in the tropic and subtropic region GPT2 underestimates the ZWD over the continents and overestimates it along the coast lines. On a global scale these effects are widely compensated and GPT2 shows no bias with respect to ray-traced ZWDs (see Table 3).

Since the hydrostatic model of GPT2w is identical to that of GPT2, small differences in ZHD are only affected by the higher spatial resolution of $1^\circ \times 1^\circ$. Nevertheless, GPT2w profits from the improved wet delay model and the additional parameter and provides ZHDs and ZWDs on a global grid with almost no bias and the smallest standard deviation (with respect to the other tropospheric blind models).

The comparison with ray-tracing data widely confirms the results from the comparison with IGS data in the previous section. Due to high variability of the ZWD it is more difficult to predict it from blind models. This is reflected in the wet standard deviation which is in all models approximately twice as high as for the hydrostatic delay.

So far we have only considered integral values of the ZWD at surface level. Since the troposphere blind models should be applicable for aviation, the performance at higher altitudes has to be guaranteed, too. If the parameter λ is defined in a proper way, the remaining ZWD at certain height levels should agree with the ZWD derived by ray-tracing. Figure 6 shows the remaining ZWD at an altitude of 10 km. Almost no water vapor remains at such heights. The global average of ZWD derived by ray-tracing is 0.3 mm with a maximum of 3.2 mm over the tropic region. RTCA MOPS, based on the rather simple set of input parameters, might be scaled to these heights. With a global average of 1.6 mm and a maximum of 2.8 mm it is quite close to the ray-traced data but takes no longitude-dependent effects into account. GPT2 - based on the rather simple wet Saastamoinen model [3] and constant specific humidity with height - overestimates the ZWD at these altitudes significantly. The global bias between GPT2 and ray-tracing is 45 mm with a maximum of 130 mm. In contrast, the improved GPT2w model profits from the advanced wet delay model and the additional input parameters T_m and λ which allow for describing the vertical distribution of the water vapor more reliably. The global bias between GPT2w and ray-tracing is 0.1 mm and therefore negligible.

Another important characteristic of a troposphere blind model is its applicability for low elevation angels. Currently the cut-off elevation angle for

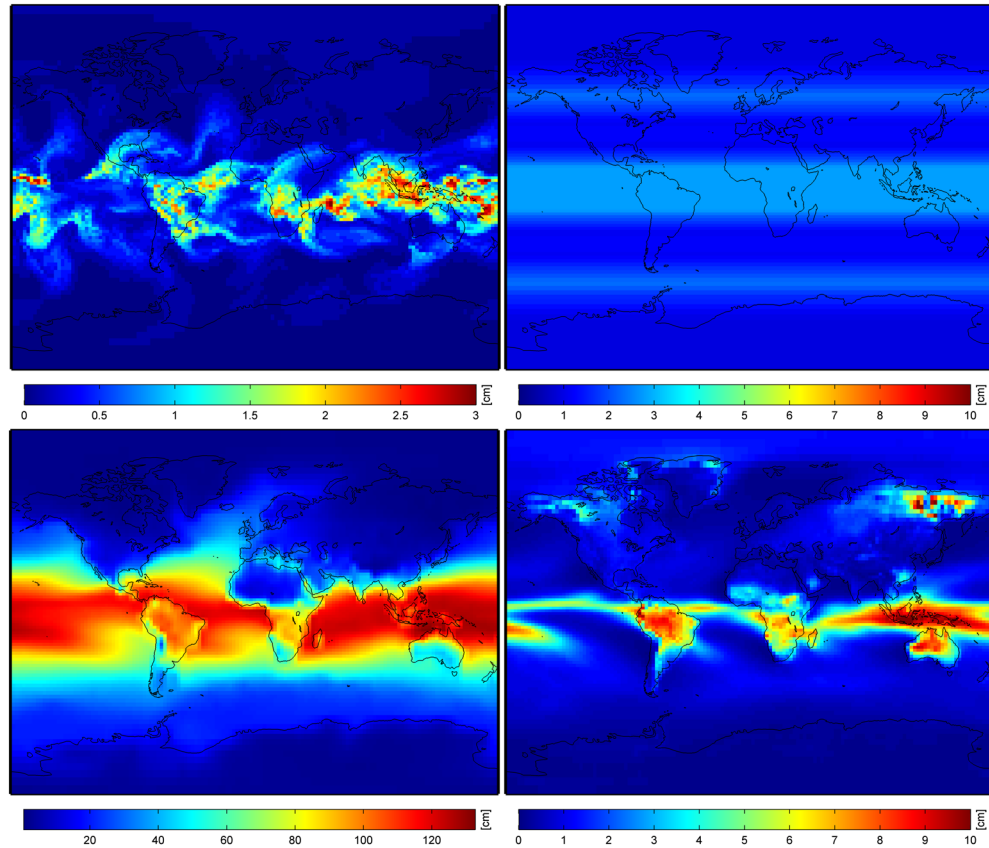


Fig. 6—Remaining ZWD [mm] at 10 km altitude derived by ray-tracing (top left), RTCA MOPS (top right), GPT2 (bottom left) and GPT2w (bottom right) for January 1st, 2013, 0:00 UT

most GNSS applications is set to 5 deg or above. For specific navigation purposes it might be useful to apply the mapping function for lower elevation angles. In order to evaluate the performance of RTCA MOPS, the ESA model, and GPT2 (GPT2w uses the same mf as GPT2) under such conditions its mapping functions have been computed for a set of elevation angles and compared with ray-tracing data. Figure 7 shows the mapping function error (dTD) for all blind models at geometric elevation angles as low as 2 deg (with 3 deg as the lowest initial elevation angle).

$$dTD(E_0) = STD_R(E_0) - ZHD_R \cdot mf_h(E_0) - ZWD_R \cdot mf_w(E_0) \quad (7)$$

The zenith hydrostatic and wet delays, ZHD_R and ZWD_R , and the slant total delay STD_R are derived by ray-tracing, E_o is the outgoing (vacuum) elevation angle of the corresponding slant range vector, and mf_h and mf_w are values of the hydrostatic and wet mapping function – calculated from RTCA MOPS, the ESA model, and GPT2, respectively.

For low elevation angles RTCA MOPS and the ESA model have a similar standard deviation. At 5 deg elevation angle it is about 7 cm and already twice as high at 3 deg elevation angles. However, in contrast to the ESA model, RTCA MOPS has a significant bias which is 10 cm at 5 deg and increases

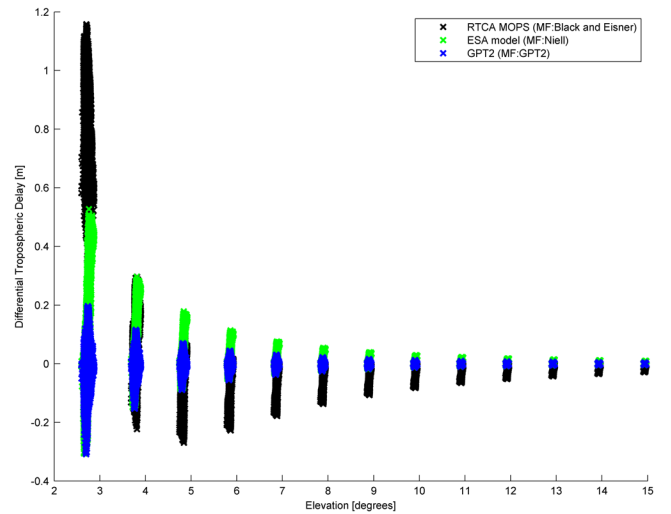


Fig. 7—Mapping function errors - difference in STD between ray-tracing and RTCA MOPS (black), ESA model (green) and GPT2 (blue) for January 1st, 2013, 0:00 UT

rapidly to about 80 cm at 3 deg. Hence RTCA MOPS should not be applied for elevation angles below 5 deg.

GPT2 and the Niell mapping function [8] have almost no bias with respect to ray-tracing. With a standard deviation of 6 cm at 3 deg and a bias of 2 cm GPT2 fits best to the ray-tracing derived STDs.

Nevertheless, below 3deg even GPT2 is not applicable anymore. More advanced mapping concepts must be considered for these purposes.

CONCLUSIONS

We have compared the tropospheric blind models RTCA MOPS, ESA model, GPT2, and GPT2w with respect to their ability to model the ZHD, ZWD, and their variations on a global scale and for selected sites. In addition we have tested the applicability of its mapping functions for low elevation angles and have found significant differences in performance quality.

The simplest and oldest model RTCA MOPS is based on tabulated data which are already outdated. Nevertheless it still shows a reasonable performance – especially over Europe, parts of Asia, and North America. Main limitations are seen over the southern hemisphere because RTCA MOPS is based on the U.S. Standard Atmosphere Supplements (1966) which is tuned for the northern hemisphere only. In addition, RTCA MOPS assumes a fixed day of maximum winter. This leads to a higher bias and standard deviation - especially in higher latitudes. With a standard deviation of 2.3% of the ZTD it is rather worse in comparison to other state-of-the-art blind models. The rather simple mapping function implemented in RTCA MOPS is applicable for 5 deg angles but only with a significant bias at lower elevation angles.

In comparison to RTCA MOPS, the ESA model profits from the more advanced climatological dataset, the improved wet delay model, and the more advanced mapping function. It fits better over most parts of the world – especially over North Africa and southern latitudes. The validation by NWM and IGS data has shown that the ESA model is able to model the ZWD and ZHD variations properly but underestimates the ZTD over the Asia-Pacific region and over South America which leads to a larger global bias. It would benefit from an update of the climatological dataset. Nevertheless, the current standard deviation can be specified with 1.8% of the ZTD which is about 20% better than for RTCA MOPS. The implemented Niell mapping function reduces the bias with respect to ray-tracing at low elevation angles but still models regional variations insufficiently.

The Global and Temperature model 2 (GPT2) is based on a climatological dataset - derived from actual monthly mean profiles from 10 years of ECMWF ERA Interim data. Hence it shows the smallest mean bias in comparison to ray-tracing and IGS data. Semi-annual harmonics allow for better taking into account the characteristic of the tropical climate which is dominated by semi-annual rain periods. The hydrostatic model of GPT2 is slightly better than the hydrostatic

ESA-model - particularly in higher latitudes. The performance of the wet delay model is worse than for the ESA model - especially in the tropics and subtropics. Hence the current standard deviation can be specified with 2.0% of the ZTD which is slightly larger than for the ESA model. The implemented mapping function shows significant improvements in comparison to the Niell mapping function. Internally stored dry and wet mapping function coefficients help to reduce the mapping function error - especially for low elevation angles down to 3 deg.

The tropospheric correction model GPT2w is still under development. First results have shown its potential to describe the tropospheric delay and its variation at any position on Earth highly reliably. Its standard deviation and in particular its bias with respect to IGS ZTDs and ray-traced derived ZHDs and ZWDs is in most cases smaller than for other blind models. This leads to a standard deviation of 1.7% of the ZTD which is slightly better than for the ESA model. Additional analysis on a longer time scale and under extreme weather conditions is necessary to finalize its development and to apply it in critical systems (e.g., safety-of-life or traffic control navigation systems). Further improvements are expected if the climatological parameters are derived from regional NWM or if the tropospheric model is operated in augmented- or site-mode (with information about the current state of the atmosphere). Nevertheless, a solution must be found to fit the improved troposphere model to the available bandwidth of an SBAS GEO. Advanced concepts in this respect are under investigation.

ACKNOWLEDGMENTS

This work has been carried out in the framework of the project TROPSY (Assessment Techniques of Tropospheric Effects for Local Augmentation Systems) together with our project partner TeleConsult Austria GmbH (TCA) and the Central Institute for Meteorology and Geodynamics (ZAMG). TROPSY is funded by ESA in the frame of the TRP (Technology Research Programm). We would like to thank Antonio Martellucci and Raul Orus Perez at ESA/ESTEC and Armin Hofmeister at Vienna University of Technology for their valuable contribution.

REFERENCES

1. Collins, J. P., "Assessment and Development of a Tropospheric Delay Model for Aircraft Users of the Global Positioning System," *Department of Geodesy and Geomatics Engineering Technical Report No. 203*, University of New Brunswick, Fredericton, New Brunswick, Canada, 1999, 174 pp.

2. RTCA, "Minimum Operational Standards for Global Positioning System/Wide Area Augmentation System Airborne Equipment," *RTCA/DO-229 B*, Washington, D. C., 1999.
3. Saastamoinen, J., "Atmospheric Correction for the Troposphere and the Stratosphere in Radio Ranging Satellites," *Geophysical Monograph Series*, 1972, pp. 247–251.
4. Askne, J. and Nordius, H., "Estimation of Tropospheric Delay for Microwaves from Surface Weather Data," *Radio Science*, Vol. 22, No. 3, 1987, pp. 379–386.
5. Black, H. D. and Eisner, A., "Correcting Satellite Doppler Data for Tropospheric Effects," *Journal of Geophysical Research*, Vol. 89, 1984, pp. 2616–2626.
6. ESA – Galileo, "Galileo Reference Troposphere Model for the user receiver," *ESA Document*, ESA-APPNG-REF/00621-AM, ver. 2.7, 2012.
7. Gibson, J. K., Kållberg, P., Uppala, S., Hernandez, A., Nomura, A., and Serrano, E., "ERA-15 Description," *ERA-15 Project Report Series*, No. 1, 2004.
8. Niell, A. E., "Global Mapping Functions for the Atmosphere Delay at Radio Wavelengths," *Journal of Geophysical Research*, Vol. 101, No. B2, 1996, pp. 3227–3246.
9. Lagler, K., Schindelegger, M., Böhm, J., Krásná, H., and Nilsson, T., "GPT2: Empirical Slant Delay Model for Radio Space Geodetic Techniques," *Geophysical Research Letters*, Vol. 40, 2013, pp. 1069–1073.
10. Böhm, J., Heinkelmann, R., and Schuh, H., "Short Note: A Global Model of Pressure and Temperature for Geodetic Applications," *Journal of Geodesy*, Vol. 81, No. 10, 2007, pp. 679–683.
11. Karabatic, A., Weber, R., and Haiden, T., "Near Real-Time Estimation of Tropospheric Water Vapour Content from Ground Based GNSS Data and its Potential Contribution to Weather Now-Casting in Austria," *Advances in Space Research*, Vol. 47, 2011, pp. 1691–1703.
12. Böhm, J., Werl, B., and Schuh, H., "Troposphere Mapping Functions for GPS and Very Long Baseline Interferometry from European Centre for Medium-Range Weather Forecasts Operational Analysis Data," *Journal of Geophysical Research*, Vol. 111, No. B02406, 2006, pp. 1–9.
13. Böhm, J., Niell, A., Tregoning, P., and Schuh, H., "Global Mapping Function (GMF): A New Empirical Mapping Function based on Data from Numerical Weather Model Data," *Geophysical Research Letters*, Vol. 33, No. L07304, 2006, pp. 1–4.
14. Dach, R. and Jean, Y., "International GNSS Service," *Technical Report*, 2012.
15. Byram, S. and Hackman, C., "Computation of the IGS Final Troposphere Product by the USNO," *IGS Workshop*, Olsztyn, Poland, July 2012.
16. Nafisi, V., Madzak, M., Böhm, J., Schuh, H., and Ardalan, A. A., "Ray-Traced Tropospheric Delays in VLBI Analysis," *Radio Science*, Vol. 47, No. RS2020, 2012.
17. GSTB-V1 Stand-alone Test Case 3, "Integration of Galileo SISA/IF with Advanced User Algorithms, Experimentation Results STC-6," 2004.